Journal of Electrical Engineering, Vol. 74, No. 6, 2023, pp. 463-473

sciendo

PAPERS

Preparation and characterization of graphene-based fluorine doped tin dioxide thin films via spray pyrolysis technique

Sherif A. Khaleel[1,*], Mahmoud Shaban[2,3], Mohammed F. Alsharekh[3], Ehab K. I. Hamad[2], and Mohamed I. M. Shehata[1]

In this work, fluorine-doped tin oxide (FTO) and graphene/fluorine-doped (G-FTO) thin films were prepared using a low-cost spray pyrolysis method at a substrate temperature of 500 °C. For the FTOs, stannous chloride was dissolved in methanol and acetic acid to form the precursor solution. A 0.05 mole (M) of hydrofluoric acid was added to the precursor as an n-type impurity. The FTO thin film has an optical transmittance of 82% and electrical sheet resistance of 15 Ω/□. By meticulously integrating graphene into the optimal precursor solution of FTO, a significant improvement in the electrical conductivity of the prepared samples was achieved, leading to a reduction in the sheet resistance to 8 Ω/□ with a suitable optical transmittance of 79%. Structural, morphological, optical, and electrical properties of the prepared sample are investigated using X-ray diffraction, scanning electron microscope, UV spectroscopy, and four-point probe technique. The best performance of the FTO thin films is achieved utilizing 2.5 μmole/L of fluorine concentration at a substrate temperature of 500°C for a spraying exposer time of 20 min. The prepared sample has an electrical sheet resistance of 15 Ω/□, optical transmittance of 82%, and figure-of-merit of 91.2×10^{-4} Ω^{-1}.The addition of 0.4 μmole/L of graphene to the optimum FTO samples enhances the performance by a remarkable reduction in the electrical the sheet resistance to 8 Ω/□ and an acceptable reduction in the optical transmittance of 79%. The overall value of the figure-of-merit increased to 118.3×10^{-4} Ω^{-1}. The achieved results offer a high potential for adopting the prepared films for electronic and optoelectronic applications.

Keywords: fluorine-doped tin-oxide, graphene/fluorine-doped tin-oxide, nebulizer spray pyrolysis technique, sheet resistance, transmittance

1 Introduction

Recently, transparent conducting oxide (TCO) thin films inhabit an enormous area in the field of optoelectronic devices owing to their distinctive properties such as high electrical conductivity and visible light transparency [1-5]. SnO_2 has been identified as a particularly suitable transparent conducting oxide material due to its chemical stability, hard mechanical properties, and ability to withstand elevated temperatures. [6]. An effective method to further improve the electrical and optical properties of SnO_2 is doping with foreign impurities such as fluorine, antimony, thorium, indium, *etc* [7]. Fluorine-doped tin-oxide (FTO) has been recently been used in many applications such as protective and anti-reflection coating, gas sensors, photovoltaic cells [8], and liquid crystal display (LCD) as transparent electrodes [9]. SnO_2:F thin films can be synthesized by various techniques. The most commonly used techniques include chemical vapor deposition [10], radio-frequency magnetron sputtering [11], sol-gel [12], pulsed laser deposition [13], and spray pyrolysis deposition technique [14]. Seeking the most reliable and economical deposition technique is a considerable goal. Among these fabrication methods, spray pyrolysis is a convenient, low-cost, and powerful tool to produce various kinds of thin films. When compared to other methods of deposition, spray pyrolysis has several benefits, such as its simplicity, affordability, reproducibility, high growth rate, applicability to mass production, and the capability to uniformly coat large areas for industrial optoelectronic applications [3].

In this work, fluorine-doped tin oxide and graphene-fluorine-doped tin oxide (G-FTO) thin films were fabricated using the spray technique to improve both electrical and optical properties. The graphene addition to the main precursor of FTO enhances the overall performance of the prepared thin films. The high electrical conductivity and optical transparency of the prepared sample of FTO and G-FTO push it to be a good candidate in solar cell applications. The transparent conducting oxide (TCO) layer such as FTO, ITO and ZnO is a very important layer in solar cells. It must have a high electrical conductivity to collect the generated current and high optical transmission to pass a larger amount of the

[1]College of Engineering and Technology, Arab Academy for Science, Technology and Maritime Transport, Aswan 81511, Egypt
[2]Electrical Engineering Department, Faculty of Engineering, Aswan University, Aswan 81542, Egypt
[3] Department of Electrical Engineering, College of Engineering, Qassim University, Unaizah 56452, Saudi Arabia
*sherif.abdalla@aast.edu

https://doi.org/10.2478/jee-2023-0054, Print (till 2015) ISSN 1335-3632, On-line ISSN 1339-309X

incident sun light. In this work, the influence of fluorine and graphene concentrations on the morphological structure, electrical, and optical properties of the produced thin films is being studied in detail. High-quality FTO and G-FTO thin film coats prepared at optimal preparation conditions could be used in optoelectronic applications efficiently.

2 Experimental work

2.1 Preparation of spray solution

Fluorine-doped tin-oxide thin films grown on glass substrates are prepared using a nebulizer spray technique at a temperature of 500°C. The initial solution is prepared by dissolving 2 g of stannous chloride ($SnCl_2$:$2H_2O$) in methanol as a solvent and glacial acetic acid (Sigma Aldrich) as an ionizing agent. The fluorine doping as an n-type dopant is achieved by adding 0.05M of hydrofluoric acid to the preliminary solution. The combination is agitated at 70°C for one hour in a sealed vessel until the powders have been fully dissolved. The glass substrates are cleaned by utilizing a combination of deionized water and methanol with the assistance of ultrasonication for 30 minutes.

Graphene is composed of a single layer of carbon atoms arranged in a hexagonal lattice. The material exhibits incredibly strong and lightweight properties. Moreover, it shows excellent electrical and thermal conductivity making it a promising candidate for a wide range of applications, including electronics, energy storage, and biomedical devices. Graphene is often referred to as the “basic building block” of many other carbon-based materials, including carbon nanotubes, fullerenes, and graphite. Its unique properties make it an exciting area of research, with many potential applications yet to be discovered [15-16]. In recent years, there has been a fast-growing interest in the use of graphene due to its electrical, optical, mechanical, and thermal properties [17-18]. A wide range of applications are using graphene specifically in the 6G wireless communication systems and the terahertz frequency band [19-20]. Practically, graphene could be synthesized in various ways on different substrates. This study involves the preparation of a highly concentrated surfactant dispersion of graphene through ultrasonication and centrifugation. The critical parameters affecting the concentration and dispersion quality are graphite concentration, surfactant concentration, ultrasonication time, and centrifugation rate. The resulting graphene exhibits exceptional electrical conductivity, enabling its utilization for enhancing the electrical properties of FTO samples. Consequently, the G-FTO films demonstrate low electrical sheet resistance without compromising optical transparency, even at minimal graphene loading.

2.2 Thin film deposition

The obtained solution is sprayed on a heated substrate using the Nebulizer, which converts the liquid to mist rather than other spray techniques that produced a huge number of small droplets. So, the prepared films are more homogenous and uniform. The prepared samples of FTO and G-FTO are grown at different times of deposition ranging from 5 to 40 minutes. The optimum time of deposition is 20 min at a constant substrate temperature of 500 °C. The spray will be processed layer by layer with a 5 min interval between each one. The substrate is heated incrementally to the requisite temperature, and the deposition process is allowed to cool at a natural rate to the ambient temperature on a heated plate.

2.3 Measurement and characterization procedures

The structural characteristics of the produced films were investigated by employing X-ray diffraction (XRD) (Philips) with Cu-Kα radiation (wavelength 1.540 Å). The film's surface morphology was inspected using a scanning electron microscope (SEM, JEOL JSM-6360 LA). The four-point probe procedure is utilized to characterize the electrical resistivity of the deposited samples. Ultraviolet-visible spectroscopy is utilized to quantify the optical transmittance within a wavelength range of 300 to 900 nanometers.

3 Results and discussions

Many parameters can affect the formation of the prepared films of FTO and G-FTO. These parameters are classified into two categories, which are fixed and variable parameters. The fixed parameters were kept constant during the preparation process such as the solution flow rate (1.5 mL/min.), the substrate temperature (500 °C), and the separated distance between the Nebulizer aperture and the sample (5 cm). On the other hand, there are two variables’ parameters: concentration of the solution and the time of deposition. For the solution concentration, more than one sample of FTO and G-FTO are prepared at different fluorine concentrations (2, 2.25, 2.5, 2.75, and 3 μmole/L) and different graphene concentrations (0.2, 0.3, 0.4, 0.5, and 0.6 μmole/L). The addition of fluorine and graphene to the main solution is to enhance the electrical properties of the prepared films.

3.1 Structural properties

3.1.1 X-ray diffraction

The crystal structures of FTO and G-FTO thin films are analyzed using X-ray diffraction (XRD). The XRD patterns show different prepared samples of FTO and G-FTO thin films with different fluorine concentrations (2, 2.5 and 3 μmole/L) and different graphene concentrations (0.2, 0.4 and 0.6 μmole/L).

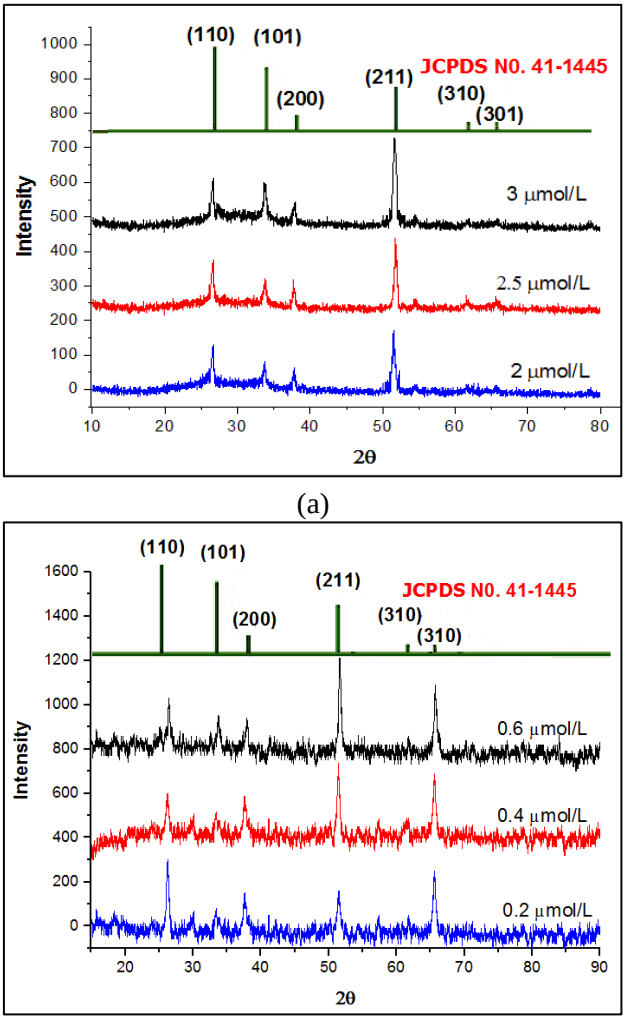

Fig. 1. XRD patterns of (a) FTO and (b) G-FTO doped thin films

The diffraction peaks reveal the polycrystalline nature of the deposited films (Database: JCPDS No. 41-1445). The observed peaks of the FTO and G-FTO thin films are (110), (101), (200), (211), (310), and (301). The FTO and G-FTO thin films exhibit a preferred orientation along the (211) diffraction plane. This dominant orientation peak intensity noticeably increases by increasing the doping level of fluorine and graphene that enhanced the crystallinity of the films as shown in Fig. 1. The lattice constant a and c of the tetragonal phase structures were computed from XRD extracted data using equations [21]

$$2d_{hkl}\sin(\theta) = n\lambda \tag{1}$$

$$\frac{1}{{d_{hkl}}^2} = \frac{h^2+k^2}{a^2} + \frac{l^2}{c^2} \tag{2}$$

where d_{hkl} is the inter-planar distance, (hkl) are the Miller indices, and a and c are the lattice parameters for the tetragonal structure. Their values, listed in Tab. 1, were in good agreement with the standard values of the refereed database.

Table 1. Parameters of prepared samples of FTO and G-FTO: inter-planar distance, lattice parameters, grain size, dislocation density, and film thickness extracted for different doping concentrations

Concentration μmole/L		d_{hkl} (Å)	Lattice parameters		Grain Size D (nm)	$\delta\times10^4$ (nm^{-2})	Thickness (nm)
			a (Å)	c (Å)			
FTO	2	1.76	4.71	3.21	37.2	7.22	238
	2.5	1.77	4.72	3.21	33.4	8.96	780
	3	1.79	4.72	3.22	29.5	11.49	1250
G-FTO	0.2	1.76	4.75	3.24	42.5	5.53	250
	0.4	1.78	4.76	3.25	38.3	6.82	813
	0.6	1.79	4.75	3.25	35.2	8.07	1320

Structure parameters such as grain size D and dislocation density δ have been evaluated also using the XRD data analysis. Deduced values of D and δ, tabulated in Tab. 1, are calculated using Scherrer's formula [22]

$$D = \frac{0.9\lambda}{\beta\cos\theta} \tag{3}$$

$$\delta = \frac{1}{D^2} \tag{4}$$

Here, λ is the X-ray wavelength 1.5405 Å, β is referred to the corresponding full-width-at-half maximum (FWHM) of the detected peak, and θ denotes the Bragg angle.

The obtained lattice parameters values *versus* concentration of the doped material of fluorine and graphene are illustrated in Fig. 2. One can observe that there is a contradiction behavior of crystalline size and the doping level. The grain size of these films has been decreased as the concentration of the doped material of fluorine and graphene increases. These reductions may be attributed to the increasing doping level preventing the movement of the grains in the main lattice and limiting the growth of the crystals. It can be observed that D and δ values are increased as the doping concentration increases, as listed in Tab. 1.

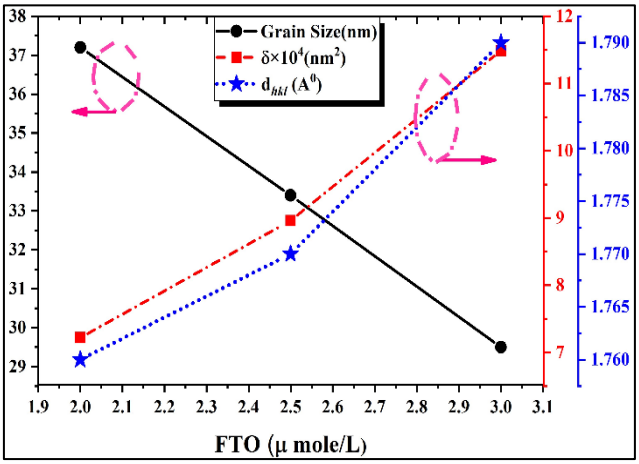

(a)

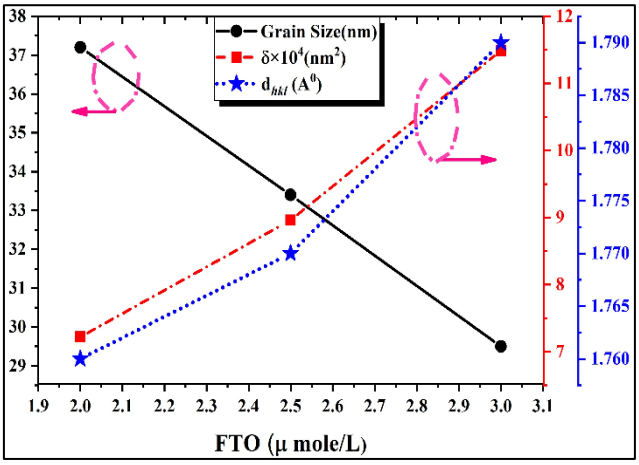

(b)

Fig. 2. Doping effect on grain size, dislocation density, and inter-planar distance

3.1.2 Morphological analysis

The surface morphology of FTO and G-FTO thin films deposited with different doping levels of fluorine and graphene concentrations are examined by SEM. The scanning electron microscopy (SEM) images presented in Figures 3 and 4 demonstrate a high degree of homogeneity and uniformity in the grain structure, accompanied by excellent crystallinity. This characteristic is expected to mitigate the adverse effects of grain boundary scattering, resulting in an increase in electrical conductivity.

Notably, the G-FTO thin films exhibit a higher surface roughness and larger grain size compared to the FTO thin films. Analysis using energy-dispersive X-ray spectroscopy (EDX) confirms the presence of distinct peaks corresponding to the elemental composition of Sn, O, F, and C in both FTO and G-FTO films, indicating that the stoichiometry of the final films remains consistent with FTO and G-FTO compositions.

3.2 Optical properties

The optical transmittance (T) curves of films with different fluorine and graphene concentrations in the wavelength range from 300 to 900 nm are depicted in Fig. 5. The average transmittance of FTO and G-FTO thin films exhibits high optical transmittance around 82% and 80%, respectively. The films demonstrate significant oscillations. This oscillation may be due to the interference phenomenon of the films with the substrate. It is observed that the optical transmission decreases with increasing the fluorine concentration in the solution. This significant reduction may be attributed to the optical scattering and the large grain sizes and boundaries. From the oscillation spectra of optical transmittance curves, the thickness of the films (t) of FTO and G-FTO are determined by using the following relation [23]

$$t = \frac{\lambda_1 \lambda_2}{2[n(\lambda_1)\lambda_2 - n(\lambda_2)\lambda_1]} \tag{5}$$

where $n(\lambda_1)$ and $n(\lambda_2)$ denotes the refractive indices of the adjacent maxima at the two wavelengths λ_1 and λ_2. In addition, the refractive index (n) can be calculated from the following equations:

$$n = \sqrt{N + \sqrt{(N^2 - n_s^2)}} \tag{6}$$

$$N = \frac{(n_s^2 + 1)}{2} + 2n_s \frac{T_{max} - T_{min}}{T_{max} \cdot T_{min}} \tag{7}$$

where n_s denotes the substrate refractive index. T_{max} and T_{min} denote the maximum and minimum transmittances at the same wavelength as depicted in transmission spectra curves (Fig. 5). The effect of fluorine and graphene concentrations on the thickness of the prepared films is listed in Table 2.

The absorption coefficient (α) can be extracted from the optical transmittance (T) using the following equation [24]

$$T = e^{-\alpha t} \tag{8}$$

where t is the thickness of the FTO and G-FTO films.

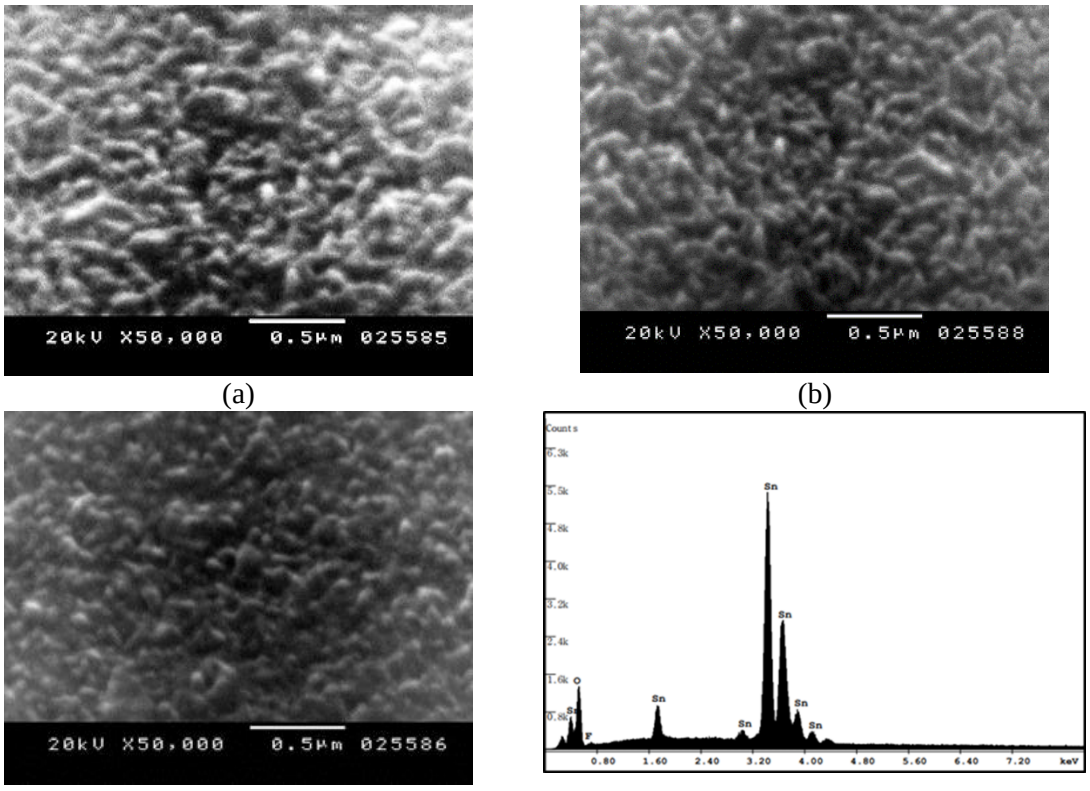

Fig. 3. SEM images and EDX spectrum of FTO: (a) 2 µmole/L, (b) 2.5 µmole/L, (c) 3 µmole/L, and (d) the EDX of FTO film

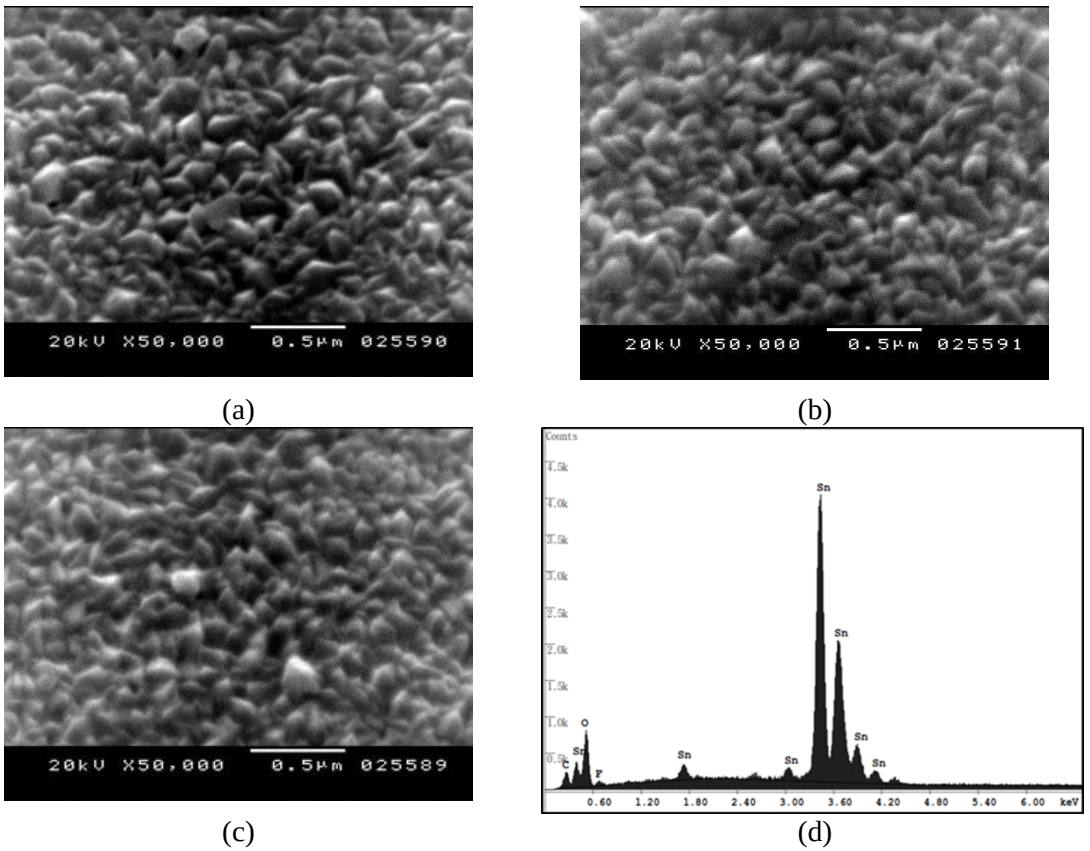

Fig. 4. SEM images and EDX spectrum of G-FTO: (a) 0.2 µmole/L, (b) 0.4 µmole/L, (c) 0.6 µmole/L, and (d) the EDX of G-FTO film

Parameter α is used to determine the optical energy bandgap E_g using the Tauc formula [24]

$$\alpha h\nu = C\left(h\nu - E_g\right)^{0.5} \quad (9)$$

where h is the Planck constant, ν is the frequency of the incident photon and C is the constant for direct transition. E_g is estimated by drawing $(\alpha h\nu)^2$ *versus* $(h\nu)$ and extrapolating the linear portion to the $h\nu$ axis at the point where $(\alpha h\nu)^2 = 0$ [25]. An increase in F doping level in SnO_2 resulted in an increased bandgap, which is consistent with previous studies. This increase is attributed to the Burstein-Moss effect, which is related to an increase in carrier concentration leading to a shift in the conduction band filling [26]. However, E_g values at high concentrations of graphene are reduced due to the low energy gap of the graphene. The energy band gap of the prepared sample of FTO and G-FTO thin films is illustrated in Fig. 6 with different fluorine ang graphene concentrations.

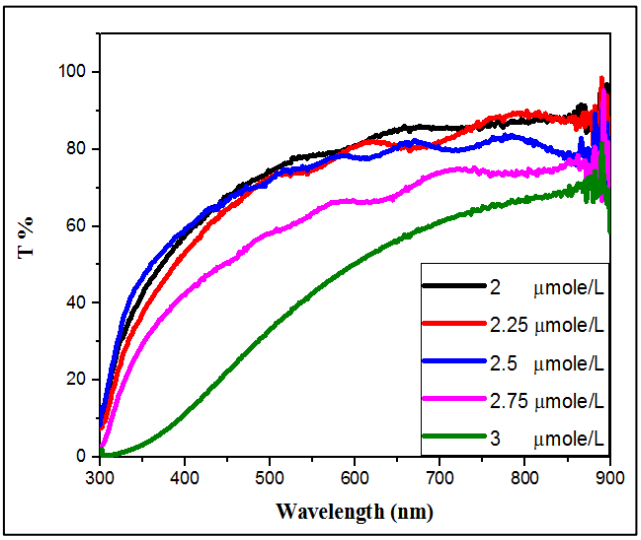

(a)

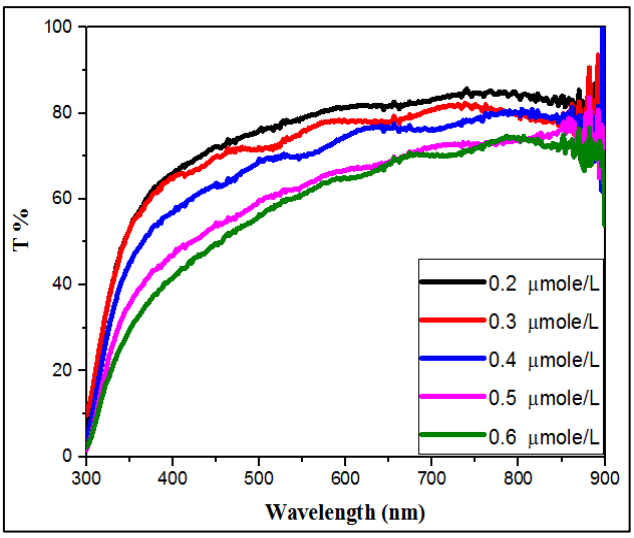

(b)

Fig. 5. Transmission spectra at different fluorine and graphene concentrations of (a) FTO and (b) G-FTO

3.3 Electrical properties

The electrical properties are the dominant parameters that attract our attention in this work. The addition of fluorine to pure SnO_2 enhances the electrical conductivity of the prepared FTO thin films. Therefore, the variations in fluorine concentration are controlling the value of sheet resistance R_{sh} measured by a four-point probe. In this procedure, the electric current I is injected through the outer two probes while the drop voltage V is measured between the inners, thus an accurate estimation of sheet resistance R_{sh} obtained by [27]

$$R_{sh} = 4.532\left(\frac{V}{I}\right) \quad (10)$$

Firstly, the sheet resistance decreases as the fluorine concentration increases until attaining a minimum value then the sheet resistance raises up again. At 2.5 µmole/L of fluorine, the lowest sheet resistance is 15 Ω/□ and increases up to 120 Ω/□ as the fluorine concentration increases up to 3 µmole/L and this result is in agreement with that obtained from optical properties [28]. In FTO thin films, F atoms substitute the O atoms in the main lattice creating extra free electrons and therefore enhancing the electrical properties of the prepared samples. The overabundant and excess of F atoms in the precursor solution increases the free carrier concentration. The motion of these carriers decreases by increasing the scattering between them leading to the increase of the sheet resistance [29].

The figure of merit (FOM) is an appropriate quantitative measure that can be used to rate the performance of the evaluated object. Measuring that can rate the performance of the evaluated object and determine its comparative effectiveness for an application. Several figures of merit have so far been defined by researchers for rating the performance of TCO which can be used for solar cells and optoelectronic applications. FOM ($\emptyset_m$) is a vital parameter in evaluating FTO thin films. It is calculated by using the Haacke formula [30]

$$\emptyset_m = \frac{T^{10}}{R_{sh}} \quad (11)$$

where T is the optical transmittance and R_{sh} is the electrical sheet resistance. According to Eqn. (11), this FOM becomes large by maximizing T and minimizing R_{sh} as shown in Table 2. The optimum preparation conditions of FTO thin films are determined using the FOM that produces high optical transmittance and low electrical sheet resistance. The optimum FTO thin film is obtained from a sample of 2.5 µmole/L fluorine concentration at 500°C of substrate temperature and 20 minutes of spraying time to give an R_{sh} value of 15 Ω/□ and T value of 82% with FOM of 91.2×10^{-4} Ω^{-1}. For the G-FTO thin films; different graphene concentrations (0.2, 0.3, 0.4, 0.5, and 0.6 µmole/L) are added to the precursor 2.5 µmole/L of the optimum FTO sample. The

addition of graphene to the main solution exhibited a significant impact on enhancing the properties of the prepared samples. The optical transmittance curves of G-FTO thin films are illustrated in Fig. 5 revealing that the addition of graphene to the FTO sample does not affect critically the optical properties that range from 70 to 85 % according to the graphene concentrations but the electrical properties of FTO thin films is the main parameter that affected by the addition of graphene to the main solution. The sheet resistance of the G-FTO thin films is reduced compared to that of the FTO as displayed in Table 2. The FOM of the prepared samples of G-FTO reveals that the optimum concentration of the graphene material that gives the best behavior (higher transmittance, lower electrical sheet resistance) is at 0.4 µmole/L of graphene concentration, 500°C of substrate temperature, and 20 min of spraying time and give an R_{sh} value of 8 Ω/□, transmittance of 79%, and FOM of 118.3×10^{-4} Ω^{-1}.

It is important to mention that R_{sh} is related to the electrical conductivity (σ) and the thin film thickness using the relation [31]:

$$\sigma = q.n.\mu \tag{12}$$

$$R_{sh} = \frac{1}{\sigma t} \tag{13}$$

where n is the free electron concentration, q is the charge of the electron and μ is the electron mobility. As the electron mobility is governed by the grain boundary scattering that is represented by [31]

$$\mu = \frac{D.q}{(2\pi m_n^* k_B T)^{1/2}} \exp\left(\frac{-\varphi_b}{k_B T}\right) \tag{14}$$

where D is the grain size, m_n^* is the effective mass of electrons, φ_b is the grain boundary potential barrier, k_B is the Boltzmann constant, and T is the temperature. In the case of the grain boundary scattering, the sheet resistance can be represented by

$$R_{sh} = \frac{1}{q.n.\mu.t} = \frac{1}{M.D} \tag{15}$$

where

$$M = \frac{n.q^2.t}{(2\pi m_n^* k_B T)^{1/2}} \exp\left(\frac{-\varphi_b}{k_B T}\right). \tag{16}$$

Equation (15) indicates an inverse relationship between the sheet resistance and the grain size of the samples. This trend agrees with results of the XRD analysis which gives a higher grain size in the G-FTO films of 38.3 nm with a lower sheet resistance of 8 Ω/□. In comparison of the FTO films give a grain size of 33.5 nm with a sheet resistance of 15 Ω/□.

This result coincides with the SEM measurements that reveal the good homogeneity and crystallinity of G-FTO samples rather than the FTO as indicated in Figs. 3 and 4.

The present study indicates that the solvent concentration can greatly affect the physical properties of FTO and G-FTO thin films. So, highly transparent conducting oxide thin films of FTO and G-FTO with low electrical sheet resistance were fabricated via the nebulizer spray pyrolysis technique. In this regard, our preparation method and proposed doping procedure introduce the material as a good candidate for optoelectronic applications. For the sake of showing the effectiveness of the proposed thin films, a comparison between recently published studies and our prepared samples of FTO and G-FTO is listed in Table 3. It is observed that the addition of graphene to the main solution enhanced the overall electrical properties while the optical transmission is not significantly affected.

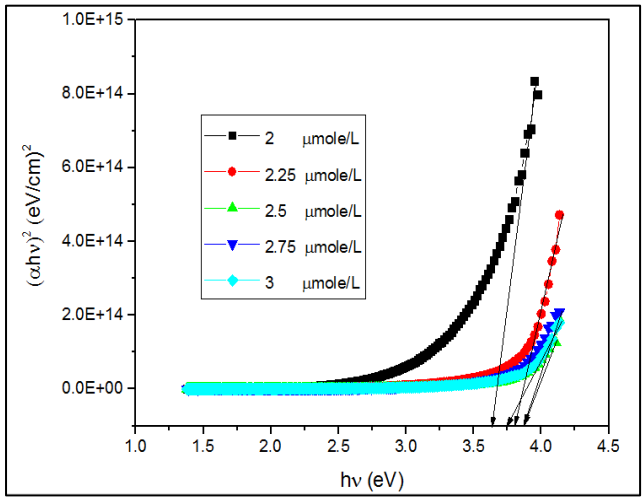

(a)

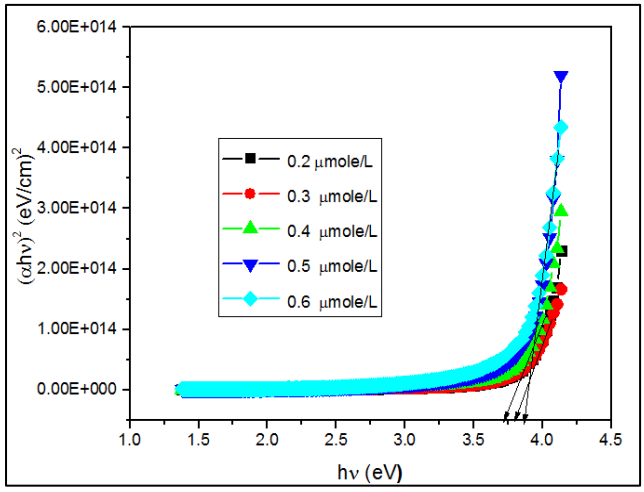

(b)

Fig. 6. Optical energy band gap at different doping levels of (a) FTO and (b) G-FTO

Table 2. Influence of doping concentration on thickness, transmittance, electrical and optical properties of FTO and G-FTO thin films

Concentration (µmole/L)		Thickness (nm)	T (%)	R_{sh} (Ω/□)	Resistivity $\rho\times10^{-6}$ (Ω.cm)	E_g (eV)	$\emptyset_m\times10^{-4}$ (Ω^{-1})
FTO	2	238	89	130	30.1	3.6	23.9
	2.25	450	85	45	20.25	3.7	43.7
	2.5	**780**	**82**	**15**	**11.7**	**3.8**	**91.6**
	2.75	966	74	50	48.3	3.9	9.8
	3	1250	66	120	150	3.7	1.3
G-FTO	0.2	250	85	45	11.2	3.7	43.7
	0.3	620	82	25	15.5	3.8	54.9
	0.4	**813**	**79**	**8**	**6.5**	**3.9**	**118.3**
	0.5	990	72	30	29.7	3.8	12.4
	0.6	1320	70	47	62.1	3.7	6.01

Table 3. Comparison of results obtained in this work to those reported in recently published reports

Ref.		thickness (nm)	T (%)	R_{sh}	E_g (eV)	$\emptyset_m\times10^{-4}$ (Ω^{-1})
[32]	G-FTO	-	77.3	26	3.69	28.3
[33]	FTO	475	81.2	24	4.01	51.9
[27]	FTO	700	81	21	3.84	57.9
[34]	FTO	320	88.5	40	3.96	73.6
[35]	FTO	-	68.5	4.5	-	50.5
[36]	FTO	620	78	-	3.75	11.5
[37]	FTO	350	85	18.9	-	130
[38]	G-FTO	300	75	372	-	15.1
Present work	FTO	780	82	15	3.8	91.6
	G-FTO	813	79	8	3.9	118.3

4 Conclusion

Special kinds of transparent conducting oxide thin films of fluorine-doped tin oxide (FTO) and graphene-fluorine-doped tin oxide (G-FTO) were successfully deposited with different fluorine and graphene concentrations at a substrate temperature of 500 °C using low-cost spray pyrolysis deposition technique. The XRD analysis exhibited that the prepared FTO and G-FTO thin films had a tetragonal structure and were polycrystalline. Scanning electron microscope images demonstrated high homogenous grains, smooth surface, and good uniformity of the deposited sample of G- FTO rather than the FTO. The measured EDX spectrum of the films showed the presence of Sn, O, C, and F elements. The optimum FTO film was obtained from 2.5 µmole/L of fluorine concentrations with 82% optical transmittance and 15 Ω/□ sheet resistance with FOM of 91.6×10^{-4} Ω^{-1}. In addition, the optimum G-FTO thin film with 79% optical transmittance, 8 Ω/□ of electrical sheet resistance, and FOM of 118.3×10^{-4} Ω^{-1} was fabricated from 0.4 µmole/L of graphene concentration. The energy bandgap due to its direct transition varied from 3.6 to 3.9 eV in the prepared samples. According to the structural, morphological, optical, and electrical properties, the prepared G-FTO film is a good candidate for optoelectronic applications.

References

[1] S. Chandra Ray, "Electrical, Electronic and Magnetic Behaviours of F-Doped SnO_2 Thin Film." *Bulletin of Materials Science*, vol. 45, no. 3, 2022, https://doi.org/10.1007/s12034-022-02739-9

[2] A. Doyan, L. Muliyadi, S. Hakim, H. Munandar, M. Taufik, "The Effect of Dopant Material to Optical Properties: Energy Band Gap Tin Oxide Thin Film." *Journal of Physics: Conference Series*, vol. 1816, no. 1, 2021, p. 012114, https://doi.org/10.1088/1742-6596/1816/1/012114

[3] C. Khelifi, A. Attaf, A. Yahia, M. Dahnoun, "Investigation of F Doped SnO_2 Thin Films Properties Deposited via Ultrasonic Spray Technique for Several Applications." *Surfaces and Interfaces*, vol. 15, 2019, pp. 244–249, https://doi.org/10.1016/j.surfin.2019.04.001

[4] H. Z. Asl and S. M. Rozati, "High-quality spray-deposited fluorine-doped tin oxide: effect of film thickness on structural, morphological, electrical, and optical properties," *Applied Physics A*, vol. 125, no. 10, Oct. 2019, doi: 10.1007/s00339-019-2943-8

[5] B. Beiranvand, A.S. Sobolev "A Proposal for a Multi-Functional Tunable Dual-Band Plasmonic Absorber Consisting of a Periodic Array of Elliptical Grooves." *Journal of Optics*, vol. 22, no. 10, Sept. 2020, p. 105005, https://doi.org/10.1088/2040-8986/abb2f3.

[6] G. Kiruthiga, K. S. Rajni, N. Geethanjali, T. Raguram, E. Nandhakumar, and N. S. Kumar, "SnO_2: Investigation of optical, structural, and electrical properties of transparent conductive oxide thin films prepared by nebulized spray pyrolysis for photovoltaic applications," *Inorganic Chemistry Communications*, vol. 145, p. 109968, Sep. 2022, doi: 10.1016/j.inoche.2022.109968.

[7] N. Suwannakham, A. Tubtimtae, and E. Wongrat, "Structural, linear/non-linear optical, optoelectrical, and electrical properties of novel crystalline antimony-doped tin oxide thin films synthesized by the chemical deposition method," *Physica B-condensed Matter*, vol. 649, p. 414440, Oct. 2022, doi: 10.1016/j.physb.2022.414440.

[8] M. A. Millán-Franco, C. A. Rodríguez-Castañeda, P. M. Moreno-Romero, J. J. Prias-Barragán, O. A. Jaramillo-Quintero, and H. Hu, "A direct correlation between structural and morphological defects of TiO_2 thin films on FTO substrates and photovoltaic performance of planar perovskite solar cells," *Materials Science in Semiconductor Processing*, vol. 161, p. 107452, Jul. 2023, doi: 10.1016/j.mssp.2023.107452.

[9] J. Liu, L. Li, Y. Um, H. Xu, C.C. Hsieh. "Optical Efficiency Modulation of Vertical Alignment Liquid Crystal Displays with Transparent Shielding and Storage Electrode." *Displays*, vol. 77, 2023, p. 102407, doi: 10.1016/j.displa.2023.102407

[10] J. Zhou, X. Tian, R. Chen, W. Chen, X. Meng. "An Ultra-Thin Chemical Vapor Deposited Polymer Interlayer to Achieve Highly Improved Stability of Perovskite Solar Cell." *Chemical Engineering Journal*, vol. 461, 2023, p. 141914, doi: 10.1016/j.cej.2023.141914.

[11] B. Zhu, H. Peng, Y. Tao, J. Wu, and X. Shi, "Highly transparent conductive F-doped SnO_2 films prepared on polymer substrate by radio frequency reactive magnetron sputtering," *Thin Solid Films*, vol. 756, p. 139360, Aug. 2022, doi: 10.1016/j.tsf.2022.139360

[12] C. Peng, Y. Li, Y. Wu, X. Zhang, M. Zou, J. Zhuang, "Electrical and optical properties of W-doped V_2O_5/FTO composite films fabricated by sol-gel method," *Infrared Physics & Technology*, vol. 116, p. 103807, Aug. 2021, doi: 10.1016/j.infrared.2021.103807.

[13] H. Latif, J. Liu, D. Mo, R. Wang, J. Zeng, P.F. Zhai, "Effect of Target Morphology on Morphological, Optical and Electrical Properties of FTO Thin Film Deposited by Pulsed Laser Deposition for $MAPbBr_3$ Perovskite Solar Cell," *Surfaces and Interfaces*, vol. 24, p. 101117, Jun. 2021, doi: 10.1016/j.surfin.2021.101117

[14] X.L. Pinheiro, A. Vilanova, D. Mesquita, M. Monteiro. "Design of Experiments Optimization of Fluorine-Doped Tin Oxide Films Prepared by Spray Pyrolysis for Photovoltaic Applications." *Ceramics International*, vol. 49, no. 8, 2023, pp. 13019-13030, doi: 10.1016/j.ceramint.2022.12.175.

[15] M. Saikia, T. Das, N. Dihingia, Y.-P. Zhao, L. F. O. Silva, and B. K. Saikia, "Formation of carbon quantum dots and graphene nanosheets from different abundant carbonaceous materials," *Diamond and Related Materials*, vol. 106, p. 107813, Mar. 2020, doi: 10.1016/j.diamond.2020.107813.

[16] W. Xiao, B. Li, J. Yan, L. Wang, X. Huang, J. Gao "Three Dimensional Graphene Composites: Preparation, Morphology and Their Multi-Functional Applications." *Composites Part A: Applied Science and Manufacturing*, vol. 165, 2023, p. 107335, doi: 10.1016/j.compositesa.2022.107335.

[17] S.A. Khaleel, E.K.I. Hamad, M.B. Saleh, "High-Performance Tri-Band Graphene Plasmonic Microstrip Patch Antenna Using Superstrate Double-Face Metamaterial for THz Communications." *Journal of Electrical Engineering*, vol. 73, no. 4, 2022, pp. 226-236, doi:10.2478/jee-2022-0031.

[18] M.Y. Shen, W.Y. Liao, T.Q. Wang, W.M. Lai, "Characteristics and Mechanical Properties of Graphene Nanoplatelets-Reinforced Epoxy Nanocomposites: Comparison of Different Dispersal Mechanisms," *Sustainability*, vol. 13, no. 4, p. 1788, Feb. 2021, doi: 10.3390/su13041788.

[19] S.A. Khaleel, E.K.I. Hamad, N.O. Parchin, and M.B. Saleh. "Programmable Beam-Steering Capabilities Based on Graphene Plasmonic THz MIMO Antenna via Reconfigurable Intelligent Surfaces (RIS) for IOT Applications." *Electronics*, vol. 12, no. 1, 2023, p. 164, doi:10.3390/electronics12010164

[20] S. A. Khaleel, E. K. I. Hamad, N. O. Parchin, and M. B. Saleh, "MTM-Inspired Graphene-Based THz MIMO Antenna Configurations Using Characteristic Mode Analysis for 6G/IOT Applications." *Electronics*, vol. 11, no. 14, 2022, p. 2152, doi:10.3390/electronics11142152.

[21] A. Rahal, A. Benhaoua, M. Jlassi, and B. Benhaoua, "Structural, optical and electrical properties studies of ultrasonically deposited tin oxide (SnO_2) thin films with different substrate temperatures," *Superlattices Microstructure*., vol. 86, Oct. 2015, pp. 403-411, https://doi.org/10.1016/j.spmi.2015.08.003

[22] R.J. Deokate, S.M.Pawar, A.V. Moholkar, V.S. Sawant, "Spray deposition of highly transparent fluorine doped cadmium oxide thin films," *Applied Surface Science*, vol. 254, no. 7, pp. 2187–2195, Jan. 2008, doi: 10.1016/j.apsusc.2007.09.006

[23] C. Gümüs, O.M. Ozkendir, H. Kavak, and Y. Ufuktepe, "Structural and optical properties of zinc oxide thin films prepared by spray pyrolysis method," *Journal of Optoelectronics and Advanced Materials*, vol. 8, no. 1, pp. 299–303, Jan. 2006, https://doi.org/10.1088/2053-1591/ab06d4

[24] Z. Y. Banyamin, P. J. Kelly, G. T. West, and J. Boardman, "Electrical and Optical Properties of Fluorine Doped Tin Oxide Thin Films Prepared by Magnetron Sputtering," *Coatings*, vol. 4, no. 4, pp. 732-746, Oct. 2014, doi: 10.3390/coatings4040732.

[25] R. Swapna, M. Ashok, G. Muralidharan, and M. C. S. Kumar, "Microstructural, electrical and optical properties of ZnO:Mo thin films with various thickness by spray pyrolysis," *Journal of Analytical and Applied Pyrolysis*, vol. 102, pp. 68-75, Jul. 2013, doi: 10.1016/j.jaap.2013.04.001.

[26] C. Guillén and J. Herrero, "TCO/metal/TCO structu-res for energy and flexible electronics," *Thin Solid Films*, vol. 520, no. 1, pp. 1-17, Oct. 2011, doi: 10.1016/j.tsf.2011.06.091

[27] A. Benhaoua, A. Rahal, B. Benhaoua, M. Jlassi, "Effect of Fluorine Doping on the Structural, Optical and Electrical Properties of SnO_2 Thin Films Prepared by Spray Ultrasonic." *Superlattices and Microstructures*, vol. 70, 2014, pp. 61-69, doi: 10.1016/j.spmi.2014.02.005.

[28] L. Chinnappa, K. Ravichandran, K. Saravanakumar, G. Muruganantham, and B. Sakthivel, "The combined effects of molar concentration of the precursor solution and fluorine doping on the structural and electrical properties of tin oxide films," *J. Mater. Sci. Mater. Electron.*, vol. 22, no. 12, 23 Apr. 2011, pp. 1827–1834, https://doi.org/10.1007/s10854-011-0369-y

[29] G. Jiang, P. Cui, Y. Liu, G. Yang, Y. Lv, C. Fu, G. Zhang., "Influence of polarization Coulomb field scattering on the electrical properties of normally-off recessed gate AlGaN/GaN metal-insulator-semiconductor high-electron-mobility transistor with ALD-Al_2O_3 gate dielectric stack," *Solid-state Electronics*, vol. 201, p. 108579, Dec. 2022, doi: 10.1016/j.sse.2022.108579.

[30] I. R. Cisneros-Contreras, A. L. Muñoz-Rosas, and A. Rodríguez-Gómez, "Resolution improvement in Haacke's figure of merit for transparent conductive films," *Results in Physics*, vol. 15, p. 102695, Dec. 2019, doi: 10.1016/j.rinp.2019.102695.

[31] M. Naftaly, S. Das, J. Gallop, K. Pan, F. Alkhalil, D. Kariyapperuma, S. Constant, C. Ramsdale., "Sheet Resistance Measurements of Conductive Thin Films: A Comparison of Techniques," *Electronics*, vol. 10, no. 8, p. 960, Apr. 2021, doi: 10.3390/electronics10080960.

[32] I.M. El Radaf, R.M. Abdelhameed. "Surprising Performance of Graphene Oxide/Tin Dioxide Composite Thin Films." *Journal of Alloys and Compounds*, vol. 765, 2018, pp. 1174-1183, doi: 10.1016/j.jallcom.2018.06.277.

[33] W.Z. Samad, M.M. Salleh, A. Shafiee, M.A. Yarmo, "Optical and Electrical Properties of Fluorine Doped Tin Oxide Thin Films." *Journal of Materials Science: Materials in Electronics*, vol. 29, no. 18, 2018, pp. 15299-15306, doi:10.1007/s10854-018-8795-8.

[34] H. Kim, R. C. Y. Auyeung, and A. Piqué, "F-doped SnO2thin films grown on flexible substrates at low temperatures by pulsed laser deposition," *Thin Solid Films*, vol. 520, no. 1, pp. 497–500, 2011. https://doi.org/10.1016/j.tsf.2011.07.025

[35] A. Purwanto, H. Widiyandari, R. Suryana, and A. Jumari, "Improving the performance of fluorine-doped tin oxide by adding salt," *Thin Solid Films*, vol. 586, pp. 41–45, 2015, https://doi.org/10.1016/j.tsf.2015.04.044.

[36] R. Thomas, T. Mathavan, M.A. Jothirajan, H.H. Somaily, "An Effect of Lanthanum Doping on Physical Characteristics of FTO Thin Films Coated by Nebulizer Spray Pyrolysis Technique." *Optical Materials*, vol. 99, 2020, p. 109518, doi: 10.1016/j.optmat.2019.109518.

[37] Z. Mahmoudiamirabad and H. Eshghi, "Achievements of high figure of merit and infrared reflectivity in SnO_2: F thin films using spray pyrolysis technique," *Superlattices and Microstructures*, vol. 152, p. 106855, Apr. 2021, doi: 10.1016/j.spmi.2021.106855

[38] C. C. Villarreal, J. I. Sandoval, P. Ramnani, T. Terse-Thakoor, D. Vi, A. Mulchandani, "Graphene Compared to Fluorine-Doped Tin Oxide as Transparent Conductor in ZnO Dye-Sensitized Solar Cells." *Journal of Environmental Chemical Engineering*, vol. 10, no. 3, 1 June 2022, p. 107551, https://doi.org/10.1016/j.jece.2022.107551

Sherif A. Khaleel received the BE and MSc degrees in electronic & communication engineering from Arab Academy for Science, Technology and Maritime Transport (AASTMT), Egypt in 2012 and 2017. He received his PhD degree in electrical engineering from Aswan University in the design of a graphene microstrip patch antenna in the THz band for 6G communication at the Faculty of Engineering, Aswan University, Aswan, Egypt. He works now as assistant professor at the college of Engineering and Technology, Department of Electronics, and communication, AASTMT, Aswan, Egypt. His current research interests include antenna design, metamaterials, 6G communication and THz materials.

Mahmoud Shaban was born in Luxor, Egypt. He received the BEng degree in electrical engineering, specializing in electronics and communications, from Assiut University, Assiut, Egypt, in 1998, the MSc degree in electronics from South Valley University, Aswan, Egypt, in 2003, and the PhD degree in applied science for electronics and materials from Kyushu University, Fukuoka, Japan, in 2009. He is currently an associate professor at Aswan University. He is also with the Department of Electrical Engineering, College of Engineering, Qassim University, Unaizah. His research interests include electronic materials, and electronic and optoelectronic devices.

Mohammed F. Alsharekh was the Head of Collage of Information and Telecommunications from 2003-2009. He is also with the Department of Electrical Engineering, College of Engineering, Qassim University, Unaizah. His research interests include electronic materials, and electronic and optoelectronic devices, material science engineering, biomedical applications, deep learning model for real time localizations, machine learning for IoT applications, and ECG application monitoring using GSM.

Ehab K. I. Hamad received the BSc and MSc degrees in electrical engineering from Assiut University, Egypt in 1994 and 1999, respectively and the PhD degree in electrical engineering from Magdeburg University, Germany in 2006. From 1996 to 2001 he was a teaching/research assistant with the Aswan Faculty of Engineering, SVU, Egypt. From July 2001 to December 2006, he was a research assistant with the Chair of Microwave and Communication Engineering, University Magdeburg. From July 2010 to April 2011, he was with the School of Computing and Engineering, University of Huddersfield, United Kingdom as a postdoctoral research assistant. He is currently full professor for antenna engineering with the Aswan University, Aswan, Egypt. He has authored or coauthored over 70 technical peer-reviewed papers in international journals and conference proceedings. He is a supervisor of about 25 master and 13 PhD theses in different universities in Egypt. His current research interests include microstrip antennas, UWB, MIMO antennas, mm-wave antennas, 5G, metamaterials. He is also interested in designing microstrip antennas using the theory of characteristic modes as well as designing antennas in the THz frequency band using graphene plasmonic material.

Mohamed I. M. Shehata received the BE and MSc degrees in Electronic & Communication Engineering from Arab Academy for Science, Technology and Maritime Transport (AASTMT), Egypt in 2004 and 2009, respectively, and the PhD degree in electrical engineering from Aswan University, Egypt in 2017. He works now as an assistant professor at the College of Engineering and Technology, Department of Electronics, and Communication, AASTMT, Aswan, Egypt. His current research interests include optical engineering, optical fiber communications, non-linear fiber optical systems, indoor and outdoor Li-Fi communications, EDFA and optical amplifier, microwave optical communications, and optical sensor for new generation of mobile communications.

Received 12 August 2023